

The Fan Design Impact on the Rotor Cooling of Axial Flux Permanent Magnet Machines

Fawzal, A. S. , Cirstea, R. M. , Gyftakis, K. , Woolmer, T. J. , Dickison, M. and Blundell, M.V.

Author post-print (accepted) deposited by Coventry University's Repository

Original citation & hyperlink:

Fawzal, A. S. , Cirstea, R. M. , Gyftakis, K. , Woolmer, T. J. , Dickison, M. and Blundell, M.V. (2016) 'The Fan Design Impact on the Rotor Cooling of Axial Flux Permanent Magnet Machines' In: International Conference on Electrical Machines (ICEM), 'XXIIth International Conference on Electrical Machines (ICEM'2016)'. Held 4-7 September 2016 at Lausanne, Switzerland. IEEE, 2725-2731.

<http://dx.doi.org/10.1109/ICELMACH.2016.7732907>

DOI 10.1109/ICELMACH.2016.7732907

ISBN 978-1-5090-2538-1

ISBN 978-1-5090-2537-4

ISBN 978-1-5090-2539-8

Publisher: IEEE

© 2016 IEEE. Personal use of this material is permitted. Permission from IEEE must be obtained for all other uses, in any current or future media, including reprinting/republishing this material for advertising or promotional purposes, creating new collective works, for resale or redistribution to servers or lists, or reuse of any copyrighted component of this work in other works.

Copyright © and Moral Rights are retained by the author(s) and/ or other copyright owners. A copy can be downloaded for personal non-commercial research or study, without prior permission or charge. This item cannot be reproduced or quoted extensively from without first obtaining permission in writing from the copyright holder(s). The content must not be changed in any way or sold commercially in any format or medium without the formal permission of the copyright holders.

This document is the author's post-print version, incorporating any revisions agreed during the peer-review process. Some differences between the published version and this version may remain and you are advised to consult the published version if you wish to cite from it.

The Fan Design Impact on the Rotor Cooling of Axial Flux Permanent Magnet Machines

A. S. Fawzal, R. M. Cirstea, K. N. Gyftakis, T. J. Woolmer, M. Dickison and M. Blundell

Abstract – Thermal management of Axial Flux Permanent Magnet (AFPM) machines is essential because it determines the machine's continuous power output and reliability. Also, thermal management is required to avoid catastrophic failure due to degradation. To help meet this challenge, a secondary cooling method can be integrated into the rotor, which can yield improved machine performance and reliability. Thermal analysis via Lumped Parameter (LM) networks is usually sufficient in predicting the thermal motor behaviour. Accuracy can be further increased with the help of Computational Fluid Dynamics (CFD), especially for devices with complex flow regions. In this paper, the fan blade was attached to the rotor of a YASA machine for flow validation, and then three different fan blade designs from other engineering applications were adopted, in order to compare the flow characteristic, power requirement and thermal characteristic for AFPM cooling applications.

Index Terms—Axial flux, Permanent magnet machines, Fluid dynamics, Rotors, Cooling, Fluid flow, Thermal analysis, CFD, SAT, Yokeless and segmented armature machine.

I. INTRODUCTION

BASED on legislation constrain; the Directive 2009/28/EC of 23 April 2009 [1] and the Commission Regulation 640/2009/EC of 22 July 2009 [2], a new development of electric machine topology with better efficiency and high energy density is needed in regard to the eco-design guideline. To meet this requirement, Axial Flux Permanent Magnet (AFPM) machine is well suited for transport and traction applications, due to its specific high power, high torque density and short axial length [3]–[5]. The advancement of this topology was made by the Segmented Armature Torus (SAT), also known as the Yokeless and Segmented Armature (YASA), that improved the torque density and efficiency over conventional AFPM machines. Derived from dual rotor AFPM torus topology,

the YASA machine combines NS and NN Torus-S topologies [6], resulting in an AFPM that is lightweight and compact in their class.

AFPM machines are categorized as disc type electrical machines that make the package compact because the stator and rotor arrangements are side-by-side. Even with modest (less complex) yet superior design topology, the internal temperature needs to be predicted during the design stage in order to avoid overheating. In general, energy conversion from electricity to mechanical motion produces losses that are manifested as heat. The operating temperature of an electrical machine can be controlled by balancing between heat generated and heat removal rate. Controlling the machine operating temperature is crucial, as this will determine its continuous power output, machine reliability and also allow to avoid any catastrophic failure caused by degradation [8]–[10]. By doing so, the maximum potential of the machine can be achieved, the life-span of the machine can be prolonged and operating life optimised. As described by Fitzgerald et al., the deterioration is a function of time and temperature [7]. Therefore, understanding of heat generation and cooling methods is required.

Extensive research on the electromagnetic analysis of AFPM machines has been done, yet limited research on the thermal aspect has been carried out [11], particularly compared to radial flux permanent magnet counterparts. Lumped Parameter (LM) networks of one-dimensional, e.g. [12], and two-dimensional, e.g. [13], approaches have been used in predicting the thermal behaviour of AFPM by compiling both solid and fluid domains. This method gives a fast solution over a broad range of machine speeds and this is why it is favourable to AFPM machine designers. However, LP method does not include any fluid domain changes related to design variation (e.g. inlet/outlet, rotor, magnet arrangement, etc.). So, Computational Fluid dynamics (CFD) modelling is required to understand the complexity of flow and thermal behaviour, at the expense of increased computational cost [14]. Furthermore, CFD can also be used to increase the accuracy of LP thermal model [15]. This is by providing heat transfer coefficients for individual components and windage losses of rotating parts in the network.

This paper presents how different rotor fan blade designs influence rotor cooling for AFPM machines, using CFD modelling, specifically considering YASA machine topology. This secondary cooling method is unique compared to conventional rotor cooling because the fan blade is attached or matted directly to the machine rotor, hence the rotor provides the air flow and dissipates the heat at the same time. The focus of this study was on fan

This work was funded and supported by Coventry University and YASA Motor Ltd., United Kingdom.

A. S. Fawzal is with the Faculty of Engineering, Environment & Computing, Coventry University, Priory Street, Coventry, CV1 5FB, UK (email: fawzala@uni.coventry.ac.uk).

R. M. Cirstea is with the School of Mechanical, Aerospace and Automotive Engineering, Coventry University, Priory Street, Coventry, CV1 5FB, UK (email: aa9340@coventry.ac.uk).

K. N. Gyftakis is with School of CEM and the Centre for Mobility and Transport, Coventry University, Priory Street, Coventry, CV1 5FB, UK (email: k.n.gyftakis@ieee.org).

T. J. Woolmer is with YASA Motors Ltd. Abingdon, Oxfordshire, OX14 4SD, UK (email: tim.woolmer@yasamotors.com)

M. Dickison is with the Faculty of Engineering, Environment & Computing, Coventry University, Priory Street, Coventry, CV1 5FB, UK (email: aa7111@coventry.ac.uk).

M. Blundell is with the Centre for Mobility and Transport, Coventry University, Priory Street, Coventry, CV1 5FB, UK (email: cex403@coventry.ac.uk).

performance, including power requirements to spin the rotor, to assess windage losses. Additionally, static temperature was evaluated, to provide insight on the heat convection of each fan blade design.

II. THE YOKELESS AND SEGMENTED ARMATURE (YASA) MACHINE AND ITS COOLING MECHANISM

Conventional AFPM machines are comprised of yokes on a rotor and stator to support the field system and protect the armature of the motor. Innovatively, the YASA machine topology is able to increase the performance of AFPM by removing the stator yoke and implementing other design changes, as illustrated in Fig. 1. The derivation of YASA topology began with NS Torus-S topology (Fig. 1-a), then evolved by excluding the stator yoke (Fig. 1-b), as it did not seriously impact the electromagnetic behaviour of the system. In Fig. 1-c, one can see that the pitch of the teeth is enlarged and individual windings feature a high strength square coil wrapped in a bonding material. This new topology improved torque density by 20% and recorded a peak efficiency of 95% with 50% less iron in the stator compared to a conventional AFPM machine [6]. Nevertheless, the full potential of the machine is currently limited by its operating temperature, although the YASA machine achieves an improvement in peak performance. Therefore, optimisation of thermal design is required to improve the motor's reliability and to further increase its performance.

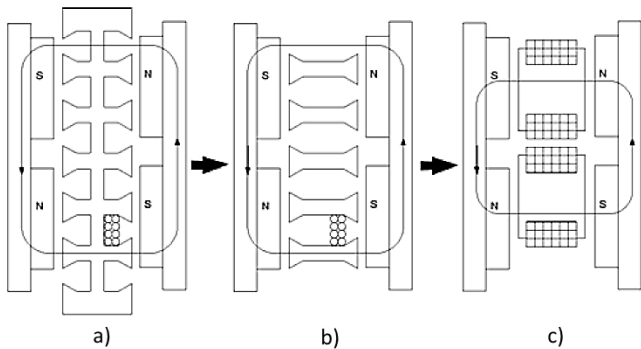


Fig. 1. YASA derivation topology begins with (a) NS Torus-S topology, (b) exclude the stator yoke and (c) other design changes [6].

The current YASA machine design uses oil as a direct stator cooling method to counter the heat generated from iron and copper losses. This is accomplished by sealing the stator assembly from the rotors and allows coolant oil to pass through between the windings. Camilleri et al. [16] have investigated this cooling method and mapped the temperature profile of YASA machine pole piece for different coolant flow rates. The study on this machine also considered the influence of stator coolant flow path geometry [17]. The findings provided sufficient thermal management for low and medium continuous power applications.

To boost up the performance of this bi-directional machine even further, a secondary cooling method has been introduced by using a rotor cooling technique. This is to

allow further thermal management on eddy currents and stray losses of the magnets and the rotor. The initial concept of rotor cooling was proposed by Vansompel [4] and the implementation of rotor cooling was shown to increase the YASA machine's continuous power by 43% and torque by 20% [18][19].

III. FAN BLADE DESIGN

The improvement of rotor cooling on the current YASA machine topology was accomplished by introducing an opening at the centre of the rotor and a single outlet on the radial cover. This is similar to the concept of a centrifugal fan, where the air will flow from the inlet through the system by a backward-inclined aerofoil blade that is attached or mated directly to the machine rotor and exits through the side outlet. This fan blade was chosen to meet specific mass flow and pressure requirements with limited understanding on its contribution towards heat transfer aspects.

For this purpose, three different fan blade designs, adopted from other engineering applications, have been selected and the flow characteristic, power requirement and thermal characteristic of each fan design have been compared. Fig. 2 shows the selection of fan blade designs, which are: Fig. 2-a, a backward-inclined aerofoil blade – from a force-draft blower application [20], Fig. 2-b, a radial aerofoil blade – from a typical fan engineering application [20] and Fig. 2-c, a tear drop pillar blade – from an automotive disc brake [21].

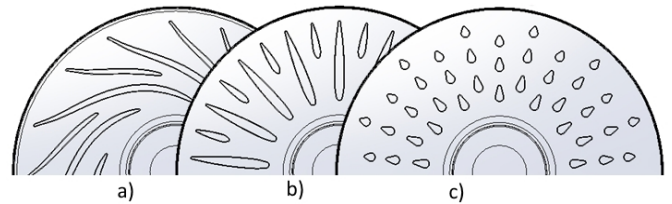


Fig. 2. The fan blade design selection with (a) backward-inclined aerofoil blade [20], (b) radial aerofoil blade [20] and (c) tear drop pillar blade [21].

IV. EXPERIMENTAL RIG

The flow measurement was carried out on a 160kW YASA machine that is in production by YASA Motors Ltd. The dimensions of the rotor inner and outer diameter are 77.0mm and 252.7mm respectively. The clearances in the system by gap ratio, s/R are: magnet-to-stator is 0.00396, rotor-to-stator is 0.02453 and rotor-to-cover is 0.00594, where s is gap distance and R is outer diameter. There was a trigger disc mounted on the rotor vanes axial surface to measure the rotational speed of the rotor and this disc also acted as a seal to avoid air spillage during operation.

For validation purposes, this machine was set to run without load, to assess the mass flow rate generated by the backward-inclined aerofoil blade, attached to the disc rotor. The machine was equipped with a dual PMF4104V mass flow sensor at the inlet opening of the machine cover, as shown in Fig. 3. The mass flow rate was recorded every 500rpm between 1000rpm to 3500rpm of rotational speed, which is equivalent to the rotational Reynolds number (Re) of $1.07e5$ to $3.73e5$ at the outer edge of the rotor disk. This

speed range was selected, based on the limitation of the mass flow sensor (limited to 600litres/min), while the nominal speed of the machine is 2100rpm. The setup was set to run until the system reached a steady state condition for mass flow rate measurement for 30seconds on every 100rpm increment with a 10rpm/s ramp rate.

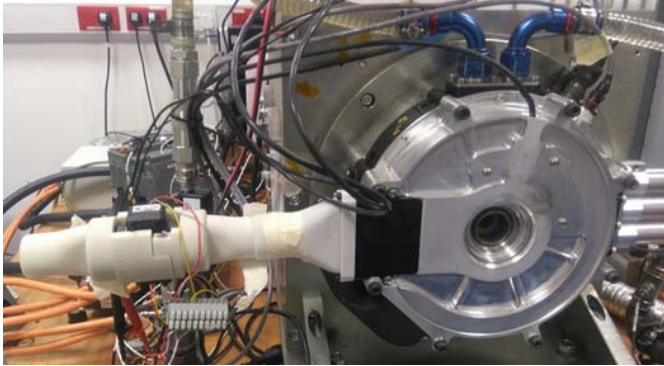


Fig. 3. The experimental rig with mass flow sensor at the inlet.

V. CFD MODEL

The complex 3D CAD design was simplified by removing features that are irrelevant to fluid flow and known to have limited or zero contribution to the flow and thermal aspects. The major CAD simplification was done using SolidWorks 2014 and the fluid volume was extracted. The 3D model was then imported into STAR-CCM+ v9.04 for further design simplification and merging the solid parts as a single solid domain. This is to include magnet circular array, rotor fan blade and trigger disc. In addition, the fluid domain was split into two parts to differentiate between static and rotational fluid domains. The static fluid domain represented the region of inlet and outlet duct, while the rotational fluid domain represented the region near to the rotor.

A complete domain of non-drive-end side was modelled, due to non-symmetrical design of inlet and outlet positions. The final CFD model included stator wall, rotor assembly, inlet duct with dual mass flow sensors and outlet extrusion (Fig. 4). Contact interface between Solid-Fluid regions and Fluid-Fluid regions was created by imprinting the mating face to allow conformal mesh between the regions.

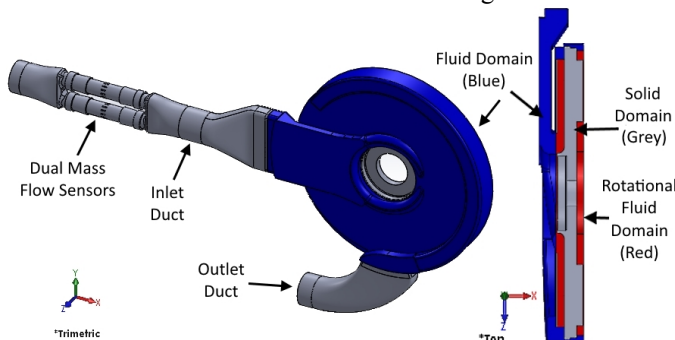


Fig. 4. CFD model including fluid domain (blue), rotational fluid domain (red), rotor & ducting (grey)

Using automated mesh generation of STAR-CCM+, an unstructured volume mesh (polyhedral cells) was used to discretise the solid and fluid domain. The prism layer was set based on the calculated dimensionless wall distance [22] of

(1)-(2) with a local Reynolds number of $3.73e5$ (3).

$$y^+ = \frac{yu\tau}{\nu} \quad ; \quad u_\tau \approx \sqrt{\frac{\bar{\tau}_w}{\rho}} \quad (1)$$

where u_τ is friction velocity near to the wall, y is first cell distance to the wall, ν is kinematic viscosity of air, ρ is air density and the wall shear stress τ_w is related to the skin friction, C_f as follows:

$$\bar{C}_f = \frac{\bar{\tau}_w}{\rho u^2 / 2} \quad (2)$$

The local Reynolds number is calculated by the rotor speed ω , rotor outer radius R and kinematic viscosity of air ν at 26.85°C of ambient temperature.

$$\text{Re}_\theta = \frac{\omega R^2}{\nu} \quad (3)$$

A low y^+ approach was used to resolve the near wall fluid region, specifically at the tight clearance area of the magnet-to-stator and the rotor-to-cover with target $y^+ \approx 1$. The average mesh count of 13million cells was produced for each one of the three fan blade designs.

Both fluid domains were set as a single physical model of air. The air was assumed to have constant density, to aid fast convergence in all simulations. This assumption was compared to the equation of state for an ideal gas and the results showed insignificant difference with longer simulation time. The inlet was set as stagnation inlet to draw air naturally by the fan rotation with 26.85°C air temperature, pressure outlet, static wall on external walls and rotational wall on the rotor walls as given in Table I. Heat input was applied at the rotor as a static temperature of 80°C , that was equivalent to the maximum allowable rotor temperature set by the machine manufacturer at full load operation.

TABLE I
BOUNDARY CONDITIONS USED FOR ALL SIMULATIONS

Boundary	Conditions
Inlet	Stagnation inlet, $p_{total} = 0 \text{ Pa}$, $T = 300 \text{ K}$
Outlet	$p_{static} = 0 \text{ Pa}$
Stator Wall	Adiabatic no-slip condition wall
Rotor Walls	No-slip condition rotating wall, $T = 353.15 \text{ K}$
Cover Wall	Adiabatic no-slip condition wall
Inlet and Outlet Duct	Adiabatic no-slip condition wall

A Moving Reference Frame (MRF) approach was applied to the rotational region to mimic rotational implicitly. This approach allowed the prediction of the rotational flow in the steady state condition and a faster solution compared to transient simulation, e.g. [23]. The rotational speed for validation was varied similarly to the experiment with a backward-inclined aerofoil blade attached. Three selections of turbulence models, namely SST (shear-stress transport) k-omega [24], Realizable k-epsilon [25] and v2-f model [26]–[29] were compared during validation. Further, the turbulence model of SST k-omega was then chosen for the comparison of the three fan blade designs.

VI. EXPERIMENTAL RESULTS AND CFD VALIDATION

The complete assembly of this machine includes a mesh-filter at the outlet to restrain any contaminant from entering the system, as a result of back-pressure. Therefore, this part was included during the experiment to evaluate its restrictiveness.

Fig. 5 shows measured mass flow rates for the ‘with’ and ‘without’ mesh-filter cases on the outlet, compared with CFD results. All turbulence models slightly under-predicted the experimental measurements with insignificant differences between them. However, the CFD models gave the same trend over the measurements. Similar results were obtained with SST k-omega and Realizable k-epsilon, while the v2-f model predicted close to measurement with mesh-filter on the outlet, although the CFD modelling did not include the mesh-filter or any porous region.

The error percentage in all turbulence models reduced at higher rotational speeds, as the flow changed to fully developed turbulent flow. The pattern of mass flow plot by CFD started to change after 2500rpm, due to the change from transitional flow and fully developed turbulent flow. Table II presents an equivalent speed study for transitional flow regime by Gregory et al. on their generic rotor-stator study [30].

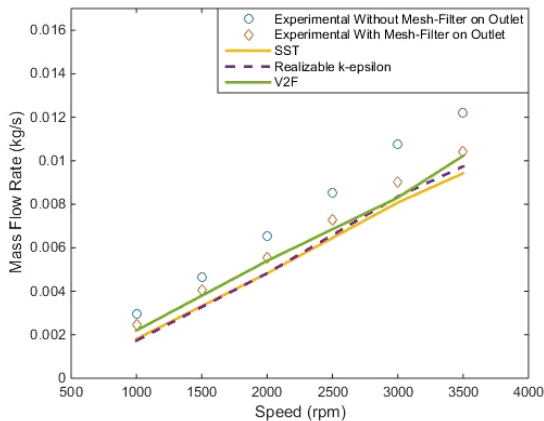


Fig. 5. Comparison CFD and experimental result of (circle) flow without mesh-filter on the outlet, (diamond) with mesh-filter on the outlet.

TABLE II

FLOW REGIME GIVEN BY GREGORY ET AL. [30] WITH ITS EQUIVALENT SPEED

Flow regime	Re	Equivalent speed
Transitional flow	$1.8e5 < Re < 2.1e5$	$1690rpm < n < 1970rpm$
Fully developed turbulent flow	$Re > 3e5$	$n > 2810rpm$

VII. RESULTS AND DISCUSSION

The SST k-omega turbulence model was chosen to assess the different performance of all fan blade designs, due to the insignificant difference of the turbulence model results shown by experimental validation (Fig. 5). Although v2-f model marks the closest to the experimental data, this model took longer time to solve because of the nonlinear relationship to express the eddy viscosity.

A. Flow Characteristic

The flow characteristic is important for rotor cooling because it shows how much air can be driven into the system to cool the rotor. Additionally, pressure development is needed to estimate the capability of suction or blowing if external ducting is required. This includes inlet ducting, outlet ducting, filters, etc.

The mass flow rate and pressure development, or pressure rise, for the three fan blades are presented in Fig. 6. A radial blade design provides the highest mass flow and pressure development compared to the other designs. The mass flow rate steadily increases, while the pressure development sharply rises as the rotational speed increases. On the other hand, the pillar type and the backward-inclined show similar characteristics on driving the mass flow and pressure development with the same relative difference across the speed range.

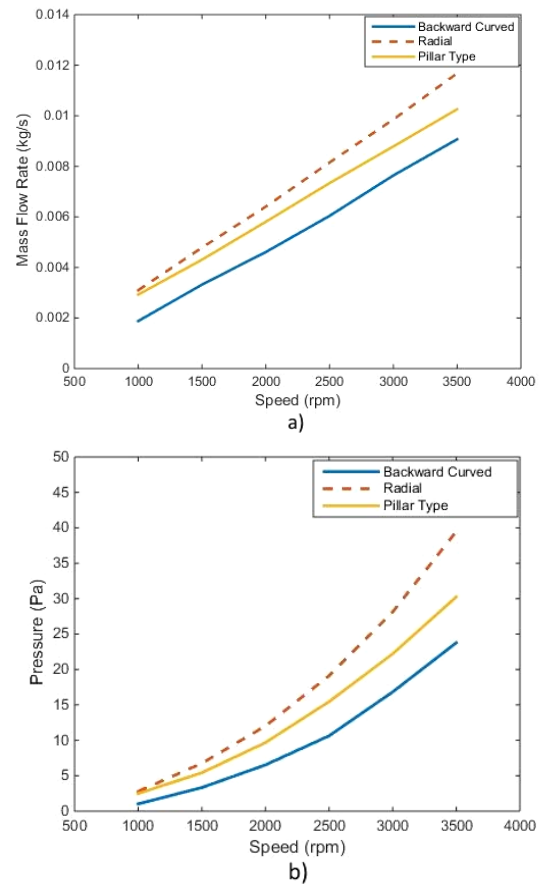


Fig. 6. a) Mass flow rate and b) pressure development of each fan design.

B. Windage Losses

In electrical machines, the fan power requirement to spin the rotor at constant speed is equal to the windage losses. This means that the net losses of windage are the sum of power requirement due to both the pressure development and shear of the air. In Fig. 7 it can be observed that the pillar type required the highest power or gives highest windage losses, followed by radial and backward-inclined.

The pressure development (Fig. 6-b) and the windage losses (Fig. 7) was normalised to the mass flow rate (Fig. 6-a). Thus Fig. 8 was introduced for each individual fan blade

design, in order to compare the fan performance.

In Fig. 8-a, the backward-inclined type provides a fair amount of pressure development across the production of mass flow rate with reasonable amount of windage losses. The fan curve of radial blade in Fig. 8-b increases sharply and is closely followed by its power curve or windage losses. However in Fig. 8-c, although the pillar type blade design is able to provide a higher amount of mass flow, compared to backward-inclined, this rotor design shows significant windage losses that increase drastically with increasing mass flow rate.

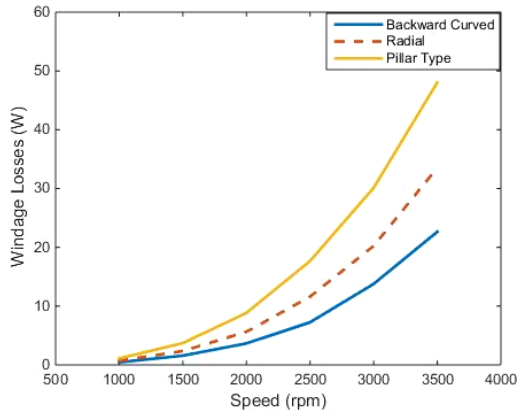


Fig. 7. Windage losses of each fan design.

C. Thermal Characteristic

The contour plot of air temperature, Fig.9, was recorded at Z +3mm above the front heated rotor surface for 3500rpm with the range between 26.85°C to 80°C. In Fig. 9-a, hot air patches at 80°C can be observed on the backward-inclined

lower aerofoil surface near to its trailing edge. This hot air then flows to the radial space of the machine, while reducing its temperature before going to, the outlet. The average air temperature at the outlet of the backward-inclined blade in Fig. 10 displays the highest outlet temperature, compared to the other design across the speed range.

Similarly, the radial blade design has multiple but smaller hot spots compared to backward-inclined blade design, as shown in Fig. 9-b. However, the hot air stays at the downwind region instead of flowing towards the machine radial space. As a result, the average air temperature at the outlet (Fig. 10) showed that, this design is the lowest in drawing the temperature out. It is also observed that, the radial blade design almost reaches its thermal steady state at 1500rpm.

On the other hand, no hot spot can be seen on the air temperature contour plot of pillar type (Fig. 9-c), yet it shows a higher temperature gradient at the radial space compared to the radial blade design. The average outlet temperature of pillar type (Fig. 10) is marked between the other fan blade designs with increasing value as the speed increases.

Furthermore, the capability of each fan design in dissipating the rotor temperature can be analysed by plotting the average air temperature within the rotating region, as presented in Fig. 11. The hot air patched of backward-inclined and radial blade (Fig. 9) proves that both designs have high average temperature within the system. However, for radial blade, this hot air remains within the system due to flow circulation at the downwind region of the blade, which made the average air outlet temperature of this design the

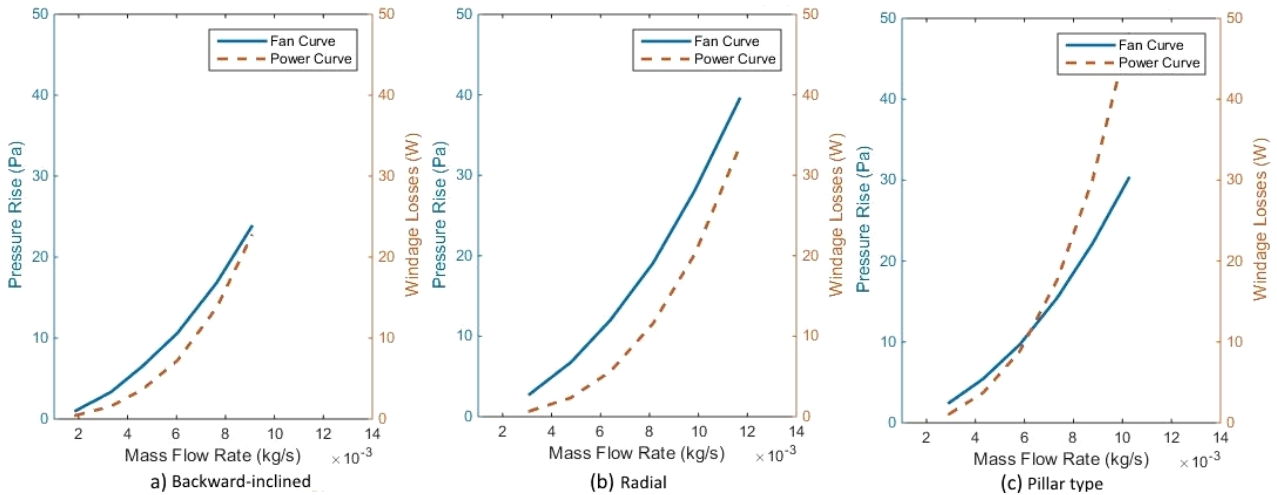


Fig. 8. Fan curve and power curve of (a) backward-inclined aerofoil blade, (b) radial aerofoil blade and (c) tear drop pillar blade.

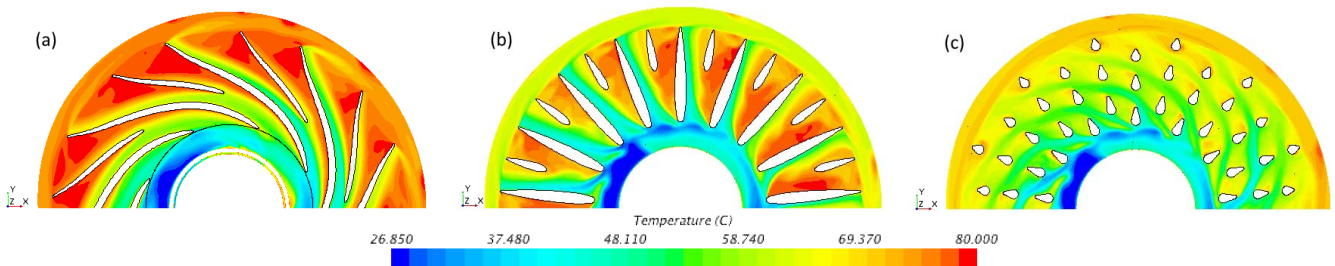


Fig. 9. Air temperature contour at z +3mm from the front heated rotor surface of (a) backward-inclined airfoil blade, (b) radial airfoil blade and (c) tear drop pillar blade.

lowest.

Based on these factors, the thermal characteristic of each fan design can be evaluated by examining the average heat transfer coefficient. The average heat transfer coefficient in Fig. 12 is calculated by the heat flux of the rotor and magnet walls divided by the temperature difference between rotor and system average temperature of Fig. 11. Fig. 12 shows that, although the backward-inclined blade design provides the lowest mass flow rate, the average heat transfer coefficient matches the radial blade because this design has the most capability in dissipating the rotor temperature. Conversely, better production of mass flow rate for the radial blade provides high heat transfer rate. Therefore, the average heat transfer coefficient is the highest, even with the lowest average air temperature flow through the outlet. Additionally, with an average mass flow rate and the least value of average air temperature within the system, the pillar type has the least quantity of the heat transfer coefficient.

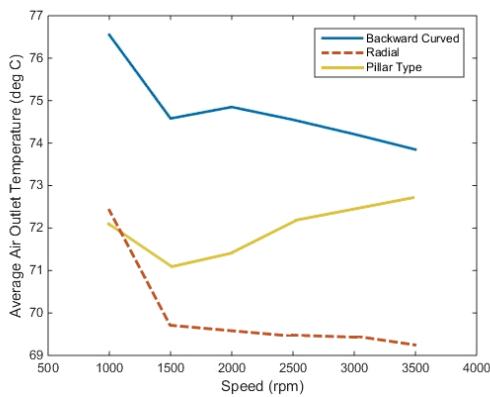


Fig. 10. Average air outlet temperature of each fan design.

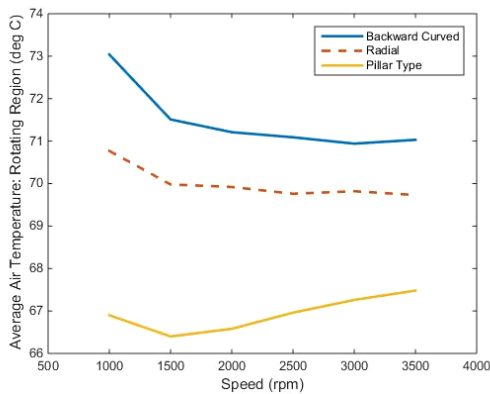


Fig. 11. Average air temperature within the rotating region.

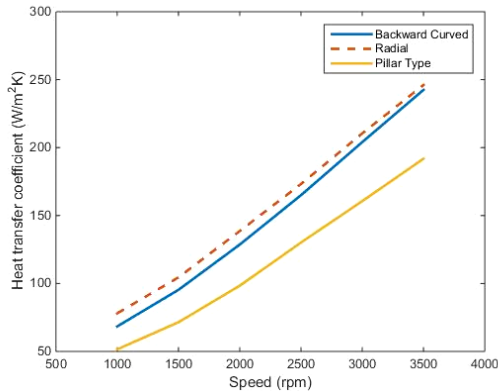


Fig. 12. Average heat transfer coefficient of each fan design.

VIII. CONCLUSION

A comparative study of different fan blade designs for rotor cooling of axial flux permanent magnet machines by CFD has been presented. Firstly, the mass flow rate from CFD and experimental measurements with three turbulence models selection was validated. It was found that the CFD modelling of mass flow rate was under-predicted and insignificantly different between the 3 tested turbulence models tested. Further validation on the thermal analysis is required in order to conclude regarding the capability of CFD modelling on predicting the heat transfer for this specific study.

The study of the characteristics of three fan blade designs has shown that each design has its own merit. Firstly, the backward-inclined design gives fair amount of flow characteristics and windage losses. Moreover, the radial design offers the highest flow characteristics with a cost of high windage losses. Finally, the pillar type needs high power requirements to provide good amount of flow characteristics. The simulation results with the same static rotor temperature have been presented to investigate the thermal characteristics of these fan blade designs. Both fan and thermal characteristics studied in this paper could be an input to a lumped parameter thermal model, in order to achieve accurate thermal losses prediction for axial flux permanent magnet machines.

In future, this study will be extended by using fixed loss densities to simulate the temperature distribution in solid domains. Further study is also required to investigate the full capability of rotor cooling techniques on AFPM machine.

IX. ACKNOWLEDGMENT

The authors would like to thank YASA Motor Ltd., Dr. Humberto Medina, Mr. Chris McCaw and Mr. David Mackenzie for their support and assistance.

X. REFERENCES

- [1] *Directive 2009/28/EC of the European Parliament and of the Council 23 April 2009*, Official Journal of the European Union, L 140/16 – L 140/62, 2009. [Online]. Available: <http://eur-lex.europa.eu/legal-content/EN/TXT/?uri=CELEX:32009L0028>
- [2] *Commission Regulation (EC) No 640/2009 of 22 July 2009*, Official Journal of the European Union, L 191/26 – L 191/34, 2009. [Online]. Available: <http://eur-lex.europa.eu/legal-content/EN/TXT/?uri=CELEX%3A32009R0640>
- [3] J. Gieras, M. Kamper and R. Wang, *Axial Flux Permanent Magnet Brushless Machines*. 2nd ed. Dordrecht: Springer Science + Business Media B.V, 2008, pp. 1-10.
- [4] H. Vansompel, "Design of an Energy Efficient Axial Flux Permanent Magnet Machine", Ph.D. dissertation, Ghent University, Belgium, 2013.
- [5] E. Odvárka, A. Mebarki, D. Gerada, N. Brown and C. Ondrůšek, "Electric Motor-Generator for a Hybrid Electric Vehicle", *Engineering Mechanics*, vol. 16, no. 2, pp. 131-139, 2009.
- [6] T. Woolmer and M. McCulloch, "Analysis of the Yokeless And Segmented Armature Machine", *2007 IEEE International Electric Machines & Drives Conference*, pp. 704 - 708, 2007.
- [7] A. Fitzgerald, C. Kingsley Jr and S. Umans, *Electric machinery*. New York: McGraw-Hill, 2003. Sixth edition. pp 668-674
- [8] D. Kothari and I. Nagrath, *Electric machines*, 4th ed. New Delhi: Tata McGraw-Hill Education, 2010, pp. 250-258.

XI. BIOGRAPHIES

- [9] K. N. Gyftakis, M. Sumislawska, D. Kavanagh, D. Howey and M. McCulloch, "Dielectric Characteristics of Electric Vehicle Traction Motor Winding Insulation under Thermal Ageing", *IEEE Transactions on Industry Applications*, early access.
- [10] M. Sumislawska, K. Gyftakis, D. Kavanagh, M. McCulloch, K. Burnham and D. Howey, "The Impact of Thermal Degradation on Properties of Electrical Machine Winding Insulation Material", *IEEE Transactions on Industry Applications*, accepted 2016.
- [11] D. Howey, A. Holmes and K. Pullen, "Prediction and measurement of heat transfer in air-cooled disc-type electrical machines", *5th IET International Conference on Power Electronics, Machines and Drives (PEMD 2010)*, pp. 1-6, 2010.
- [12] R. Wang, M. Kamper and R. Dobson, "Development of a Thermofluid Model for Axial Field Permanent-Magnet Machines", *IEEE Transactions on Energy Conversion*, vol. 20, no. 1, pp. 80-87, 2005.
- [13] C. Lim, J. Bumby, R. Dominy, G. Ingram, K. Mahkamov, N. Brown, A. Mebarki and M. Shanel, "2-D lumped-parameter thermal modelling of axial flux permanent magnet generators", *Electrical Machines, 2008. IECM 2008. 18th International Conference on*, pp. 1-6, 2008.
- [14] Y. Chong, D. Magahy, J. Chick, M. Mueller, D. Staton and A. McDonald, "Numerical modelling of an axial flux permanent magnet machine for convection heat transfer", *IET Conference on Renewable Power Generation (RPG 2011)*, pp. 1-6, 2011.
- [15] G. Airoidi, G. Ingram, K. Mahkamov, J. Bumby, R. Dominy, N. Brown, A. Mebarki and M. Shanel, "Computations on heat transfer in axial flux permanent magnet machines", *2008 18th International Conference on Electrical Machines*, pp.1-6, 2008.
- [16] R. Camilleri, T. Woolmer, A. Court and M. McCulloch, "Investigation into the temperature profile of a liquid cooled YASA® AFPM machine", *6th IET International Conference on Power Electronics, Machines and Drives (PEMD 2012)*, pp. 1-8, 2012.
- [17] R. Camilleri, D. Howey and M. McCulloch, "Predicting the Temperature and Flow Distribution in a Direct Oil-Cooled Electrical Machine With Segmented Stator", *IEEE Trans. Ind. Electron.*, vol. 63, no. 1, pp. 82-91, 2016.
- [18] *P400 Series: Compact axial flux motors and generators*, Abingdon: YASA Motors Ltd., 2016. [Online]. Available: http://www.yasamotors.com/wp-content/uploads/2015/09/YASA_P400_Product_Sheet.pdf
- [19] *YASA-400: Axial flux electric motor*, Abingdon: YASA Motors Ltd., 2016. [Online]. Available: <http://www.yasamotors.com/wp-content/uploads/2015/09/YASA-400-Product-Sheet.pdf>
- [20] H. Bloch and C. Soares, *Process plant machinery*. Boston: Butterworth-Heinemann, 1998, pp. 520-525.
- [21] L. Wallis, E. Leonardi, B. Milton and P. Joseph, "Air Flow and Heat Transfer in Ventilated Disc Brake Rotors with Diamond and Tear-Drop Pillars", *Numerical Heat Transfer, Part A: Applications*, vol. 41, no. 6-7, pp. 643-655, 2002.
- [22] H. Schlichting and K. Gersten, *Boundary-layer theory*, 8th ed. Berlin: Springer, 2000, pp. 517-522.
- [23] M. Darvish and S. Frank, "Toward the CFD Simulation of Sirocco Fans: From Selecting a Turbulence Model up to the Role of the Cell Shapes", in *FAN2012: International Conference on Fan Noise, Technology and Numerical Methods*, Senlis, France, 2016, pp. 1-12.
- [24] F. Menter, "Two-equation eddy-viscosity turbulence models for engineering applications", *AIAA Journal*, vol. 32, no. 8, pp. 1598-1605, 1994.
- [25] T. Shih, W. Liou, A. Shabbir, Z. Yang and J. Zhu, "A New K-epsilon Eddy Viscosity Model for High Reynolds Number Turbulent Flows: Model Development and Validation", *Ntrs.nasa.gov*, 1994. [Online]. Available: <http://ntrs.nasa.gov/search.jsp?R=19950005029>.
- [26] P. Durbin, "Separated flow computations with the k-epsilon-v-squared model", *AIAA Journal*, vol. 33, no. 4, pp. 659-664, 1995.
- [27] P. Durbin, "On the k-3 stagnation point anomaly", *International Journal of Heat and Fluid Flow*, vol. 17, no. 1, pp. 89-90, 1996.
- [28] F. Lien, G. Kalitzin and P. Durbin, "RANS modeling for compressible and transitional flows", in *Center for Turbulence Research - Proceedings of the Summer Program*, 1998, pp. 267-286.
- [29] L. Davidson, P. Nielsen and A. Sveningsson, "Modifications of the V2 Model for Computing the Flow in a 3D Wall Jet", *Proceedings of the International Symposium on Turbulence, Heat and Mass Transfer, October 12 - 17, 2003, Antalya, Turkey.*, vol. 4, pp. 577-584, 2003.
- [30] N. Gregory, J. Stuart and W. Walker, "On the Stability of Three-Dimensional Boundary Layers with Application to the Flow Due to a Rotating Disk", *Philosophical Transactions of the Royal Society A: Mathematical, Physical and Engineering Sciences*, vol. 248, no. 943, pp. 155-199, 1955.

Ahmad Syahid Fawzal was born in Selangor, Malaysia on November 1982. He received the Diploma of Engineering Technology in Machine Building and Maintenance from Universiti Kuala Lumpur Malaysia France Institute (UniKL MFI) (2007), continued for a BEng in Mechanical Engineering at University of Derby, UK (2009) and MSc in Computational Fluid Dynamics at Cranfield University, UK (2012)

His employment between of his study included CFD consultancy for oil & gas industry at BMT Fluid Mechanics Ltd. and machine reliability consultant (vibration) at AF Condition Monitoring (M) Sdn Bhd. He is currently a Ph.D candidate at Coventry University. His research interests include windage losses, fan performance, thermal and cooling of electrical machines.

Remus M. Cirstea was born in Brasov, Romania, on February 1979. He holds a degree in Automotive Engineering from Transilvania University, Brasov, Romania (2002) and a Master's degree in Automotive Engineering from Coventry University, UK (2009).

He then worked as a research assistant with Coventry University as part of the Low Carbon Technology Project (2010-2012) and after that he increased his commitments towards teaching undergraduate and postgraduate students. He is currently Course Director for the MSc Automotive Engineering programme at Coventry University and a lecturer in fluid dynamics. His research activities involve external aerodynamics for vehicle with focus towards the cooling drag on vehicles due to momentum loss in the airflow.

Konstantinos N. Gyftakis (M'11) was born in Patras, Greece, on May 1984. He received the Diploma in Electrical and Computer Engineering from the University of Patras, Patras, Greece in 2010.

He pursued a Ph.D in the same institution in the area of electrical machines condition monitoring and fault diagnosis (2010-2014). Then he worked as a Post-Doctoral Research Assistant in the Dept. of Engineering Science, University of Oxford, UK (2014-2015).

He is currently a Lecturer, School of Computing, Electronics and Mathematics, Faculty of Engineering, Environment and Computing and an associate with the Research Centre for Mobility and Transport, Coventry University, UK. His research activities are in fault diagnosis, condition monitoring and degradation of electrical machines. He has authored/co-authored more than 35 papers in international scientific journals and conferences.

Tim J. Woolmer was born in Oxford 1981. He holds an Engineering degree and a DPhil from Oxford University.

In 2009 he founded YASA Motors Ltd., and now works there as the CTO. He has published a number of papers and patents on the YASA motor and related technologies. His research interests include magnetic, thermal and mechanical design

Mike Dickison was born in Farnborough, Hampshire in 1959. After completing an MSc in Automotive Product Engineering at Cranfield, he had a 23 year career working in automotive consultancies.

After initially working in the structural analysis and test fields, he subsequently led complete vehicle engineering programmes with responsibility for both technical and commercial aspects. For the past 7 years Mike has been working at Coventry University, where he is an Associate Dean in the Faculty of Engineering, Environment & Computing. Mike's research interests include lightweight structures and low carbon vehicle technologies.

Mike Blundell is well known for his work in vehicle dynamics and the use of multi-body systems (MBS) software. Prior to joining the University he worked for the ship and submarine design department of the Ministry of Defence and for Boeing (Europe). During the 1980s he was an early user of ADAMS working for Tedas Ltd the original distributors of the ADAMS software in Europe. After joining Coventry University in 1991 he led their research in the vehicle dynamics area with a particular focus on tyre modelling and the efficient use of MBS software.

Major projects have included a collaborative EPSRC/Airbus project looking into aircraft tyre modelling and a European 6th Framework project considering occupant safety in Helicopter crashes. Recent and current work has involved the Niche Vehicle Project, the Low Carbon Vehicle Technology Project and European funded work modelling the protection of civil infrastructures from terrorist attacks.

